frontiers | Frontiers in Medicine

TYPE Original Research
PUBLISHED 12 June 2024
DOI 10.3389/fmed.2024.1340012

OPEN ACCESS

EDITED BY
Doron Kabiri,
Hadassah Medical Center, Israel

REVIEWED BY
David W. Walker,
RMIT University, Australia
Yijen L. Wu,
University of Pittsburgh, United States

*CORRESPONDENCE
Mike Seed
✉ mike.seed@sickkids.ca
Janna L. Morrison
✉ janna.morrison@unisa.edu.au

†These authors have contributed equally to this work

RECEIVED 07 December 2023
ACCEPTED 04 June 2024
PUBLISHED 12 June 2024

CITATION
Darby JRT, Saini BS, Holman SL, Hammond SJ, Perumal SR, Macgowan CK, Seed M and Morrison JL (2024) Acute-on-chronic: using magnetic resonance imaging to disentangle the haemodynamic responses to acute and chronic fetal hypoxaemia.
Front. Med. 11:1340012.
doi: 10.3389/fmed.2024.1340012

Acute-on-chronic: using magnetic resonance imaging to disentangle the haemodynamic responses to acute and chronic fetal hypoxaemia

Jack R. T. Darby[1], Brahmdeep S. Saini[2], Stacey L. Holman[1], Sarah J. Hammond[1], Sunthara Rajan Perumal[3], Christopher K. Macgowan[2], Mike Seed[2,4*†] and Janna L. Morrison[1,2,4*†]

[1]Early Origins of Adult Health Research Group, Health and Biomedical Innovation, UniSA: Clinical and Health Sciences, University of South Australia, Adelaide, SA, Australia, [2]Peter Gilgan Centre for Research and Learning, The Hospital for Sick Children, Research Institute, Toronto, ON, Canada, [3]Preclinical, Imaging & Research Laboratories, South Australian Health & Medical Research Institute, Adelaide, SA, Australia, [4]Department of Physiology, Faculty of Medicine, University of Toronto, Toronto, ON, Canada

Introduction: The fetal haemodynamic response to acute episodes of hypoxaemia are well characterised. However, how these responses change when the hypoxaemia becomes more chronic in nature such as that associated with fetal growth restriction (FGR), is less well understood. Herein, we utilised a combination of clinically relevant MRI techniques to comprehensively characterize and differentiate the haemodynamic responses occurring during acute and chronic periods of fetal hypoxaemia.

Methods: Prior to conception, carunclectomy surgery was performed on non-pregnant ewes to induce FGR. At 108–110 days (d) gestational age (GA), pregnant ewes bearing control ($n = 12$) and FGR ($n = 9$) fetuses underwent fetal catheterisation surgery. At 117–119 days GA, ewes underwent MRI sessions where phase-contrast (PC) and T_2 oximetry were used to measure blood flow and oxygenation, respectively, throughout the fetal circulation during a normoxia and then an acute hypoxia state.

Results: Fetal oxygen delivery (DO_2) was lower in FGR fetuses than controls during the normoxia state but cerebral DO_2 remained similar between fetal groups. Acute hypoxia reduced both overall fetal and cerebral DO_2. FGR increased ductus venosus (DV) and foramen ovale (FO) blood flow during both the normoxia and acute hypoxia states. Pulmonary blood flow (PBF) was lower in FGR fetuses during the normoxia state but similar to controls during the acute hypoxia state when PBF in controls was decreased.

Conclusion: Despite a prevailing level of chronic hypoxaemia, the FGR fetus upregulates the preferential streaming of oxygen-rich blood via the DV-FO pathway to maintain cerebral DO_2. However, this upregulation is unable to maintain cerebral DO_2 during further exposure to an acute episode of hypoxaemia. The haemodynamic alterations required at the level of the liver and lung to allow the DV-FO pathway to maintain cerebral DO_2, may have lasting consequences on hepatic function and pulmonary vascular regulation after birth.

KEYWORDS

MRI, fetus, hypoxaemia, acute hypoxaemia, chronic hypoxaemia, hypoxia, IUGR, FGR

1 Introduction

Fetal growth restriction (FGR) occurs in ~10% of pregnancies and represents a significant risk factor for both poor perinatal and neonatal outcomes (1–4). In comparison to the postnatal environment, *in utero* oxygen availability in uncomplicated pregnancies is already limited to the extent that the *in utero* environment has been described as "Everest *in utero*" (5). This relatively hypoxaemic environment is in fact normal for the developing fetus, who even at these low oxygen levels still operates with a significant safety margin of oxygen availability (6, 7) without evidence of a preference toward anaerobic metabolism (8). As such, further impairments to oxygen availability remove this safety margin and increase the risk of poor outcomes.

Fetal hypoxaemia may occur chronically as is the case with placental insufficiency induced FGR or as acute episodes such as during transient umbilical cord occlusions and myometrial contractions (9–14). The haemodynamic response to acute hypoxia is well characterised in fetal sheep (15, 16). Briefly, an initial bradycardia is followed by a rise in mean arterial pressure and peripheral vascular resistance (13, 17, 18). Importantly, this coincides with a phenomenon known as "brain sparing" whereby a redistribution of cardiac output allows for a greater proportion of oxygenated blood to be delivered to the brain (15).

Although less is known about the haemodynamic profile during chronic hypoxaemia, there is evidence that "brain sparing" still occurs. However, rather than a redistribution of cardiac output (19–21), brain sparing during chronic hypoxaemia may result more from the preferential streaming of oxygenated blood from the placenta through the unique shunts of the fetal circulation toward the brain. Moreover, even less is known about the consequences of a second acute episode of hypoxaemia upon a prolonged period of hypoxaemia (acute-on-chronic) such as that which can occur during FGR. However, there is some evidence to suggest that there may be a sensitising effect on the cardiovascular system in response to acute-on-chronic hypoxaemia (22, 23). It is therefore clear that regardless of the cause or duration of the hypoxaemic insult, intrinsic mechanisms are in place to ensure that the brain has the best opportunity for appropriate development. Unfortunately, despite these intrinsic attempts to protect brain growth, the reduced safety margin of oxygenation and the increased risk that the growth restricted fetus has for additional acute complications in late gestation (24) significantly increases the risk of hypoxaemia induced neurodevelopmental deficits (25).

Although there is a haemodynamic attempt to spare brain growth and development in response to hypoxaemia, it is now clear that the presence of brain sparing does not indicate normal cerebral development (25–28). This is particularly highlighted by the fact that over prolonged periods of hypoxaemia, such as those associated with FGR, vascular tone of the cerebral arteries normalizes and instead cerebral metabolism is downregulated (29). As such it is imperative that we better understand how an acute episode of hypoxaemia impacts both cerebral oxygen delivery (DO_2) and consumption (VO_2) in a fetus that is already chronically hypoxaemic.

We have recently validated and utilised a combination of the clinically relevant MRI techniques: cine phase-contrast (PC (30–33)) and T_2 oximetry (34–36), to thoroughly characterise the fetal circulation and better understand how these haemodynamics are influenced by vasoactive agents (37–39) and FGR in sheep (40, 41), as well as congenital heart disease, maternal sleep position and FGR in humans (20, 42–45). Herein, we aimed to apply these techniques to a well-established sheep model of early-onset FGR to determine the impact of a second hit in the form of an episode of acute hypoxia on the haemodynamics of a fetus that is chronically hypoxaemic.

2 Materials and methods

2.1 Ethical considerations

All experimental protocols were reviewed and approved by the Animal Ethics Committee of the South Australian Health and Medical Research Institute (SAHMRI) and abided by the Australian Code of Practice for the Care and Use of Animals for Scientific Purposes developed by the National Health and Medical Research Council. Ewes from the SAHMRI farm (Burra, South Australia) were housed in an indoor facility with a constant ambient temperature of 20–22°C and a 12 h light/dark cycle. Ewes were housed in individual pens in view of other sheep and had *ad libitum* access to food and water. All investigators understood the ethical principles outlined in Grundy (46) and the principles of the 3Rs, specifically the reduction of the use of animals in research (47).

2.2 Caruncletomy surgery and mating

To induce placental restriction (PR) resulting in FGR, ewes ($n = 9$) underwent caruncletomy surgery. Induction of anaesthesia in ewes was via ketamine and diazepam (7 mg/kg IV and 0.3 mg/kg IV, respectively: Lyppards Pty Ltd.). Anaesthesia was maintained with isoflurane 1.5–2% in oxygen (Provet, SA). The uterus was incised, and most caruncles removed, leaving approximately four visible in each horn of the uterus. Analgesia meloxicam; (0.5 mg/kg, subcutaneously) was administered on the day before surgery and 24 h later (48). Antibiotics were administered (525 mg procaine penicillin and 393.75 mg benzathine penicillin: Duplocillin®, Lyppards Pty Ltd.) and 250 mg dihydrostreptomycin (Sigma, St Louis, MO, United States) intramuscularly on the day of surgery. Ewes (Control and PR) were mated with a proven ram, with ultrasound to confirm pregnancy at 50–55 days (d) gestational age (GA; term, 150 days).

2.3 Fetal catheterization surgery

At 108–110 days GA, singleton bearing Merino ewes ($n = 21$; control, $n = 12$; PR, $n = 9$) underwent surgery as previously

described (49, 50). Anaesthesia was induced with intravenous diazepam (0.3 mg/kg) and ketamine (5 mg/kg) and then maintained with isoflurane (1.5–2.5% in 100% oxygen). Vascular catheters were implanted into the maternal jugular vein, fetal femoral vein, femoral artery as well as the amniotic cavity (49, 50). Ewes received an intramuscular injection of antibiotics 3.5 mL of Duplocillin (150 mg/mL procaine penicillin and 112.5 mg/mL benzathine penicillin; Norbrook Laboratories Ltd., Gisborne, Australia) and 2 mL of 125 mg/mL Dihydrostreptomycin (Sigma, St Louis, MO, United States) at surgery and for 3 days following surgery. Fetuses received an intramuscular injection of 1 mL of Duplocillin (150 mg/mL procaine penicillin and 112.5 mg/mL benzathine penicillin); and 1 mL of 125 mg/mL Dihydrostreptomycin during surgery. All ewes received meloxicam (0.5 mg/kg, subcutaneously) for analgesia on the day before surgery and 24 h later (48). Each fetus received antibiotics (500 mg; sodium ampicillin, Commonwealth Serum Laboratories) intra-amniotically for 4 days post-surgery.

2.4 Experimental protocol

Pregnant ewes underwent MRI scans between 116–119 days GA. Ewes were fasted for at least 12 h before MRI. General anaesthesia was induced in the ewe with intravenous diazepam (0.3 mg/kg) and ketamine (5 mg/kg) and maintained with 2–2.5% isoflurane (Lyppards, South Australia, Australia). The ewe was then positioned on its left side for the duration of the scan and ventilated to create normal fetal oxygen levels (respiratory rate 16–18; ~1 L O_2 and 5 L air). Maternal heart rate and arterial oxygen saturation were measured using an MRI compatible SaO_2/heart rate monitor (Nonin Medical Inc., Plymouth, United States). The sensor was placed on the pregnant ewe's teat and measurements were continuously recorded using LabChart 7 (31, 51).

The fetal femoral artery and amniotic catheters were connected to displacement transducers, a quad-bridge amplifier, and a data acquisition unit (PowerLab, ADInstruments, Castle Hill, Australia) to record fetal blood pressure (corrected for amniotic pressure). All data were sampled at a rate of 1,000 Hz, digitized, and recorded using LabChart 7 (ADInstruments, Castle Hill, Australia). The resulting fetal blood pressure signal acted as a real time cardiac trigger for fetal MRI scanning and the maternal heart rate from the sensor was placed on the pregnant ewe's teat was used as the gating signal for the uterine arteries (7, 52, 53).

Imaging was performed on a 3 Tesla clinical MRI system (MAGNETOM Skyra, Siemens Healthineers, Erlangen, Germany). Fetal vessel blood flow measurements and oxygen saturations were determined by PC and T_2 relaxometry MRI techniques, respectively, as previously described (31, 38, 54). MRI measurements were taken firstly in a normoxaemic state, in which the oxygen supply to the ewe was titrated to match fetal blood gas status as determined in the morning of the MRI day whilst the ewe was conscious (both controls and FGR). The MRI measurements were then repeated in a state of acute hypoxaemia by reducing maternal SpO_2 to ~80–85% via a reduction of oxygen and/or the addition of nitrogen into the inspired air. MRI acquisitions during the acute hypoxaemia period began 10 min after maternal SpO_2 was reduced and stable.

2.5 Determination of blood flow within the uterine arteries and the fetal circulation

The fetal femoral arterial pressure waveform was used to generate a cardiac trigger for MR imaging (52, 53). Two-dimensional cine PC imaging was performed to measure blood flow within the fetal circulation with corresponding vessel appropriate velocity encoding (VENC). PC-MRI acquisitions were completed for the ascending aorta (AAo; VENC = 150 cm/s), main pulmonary artery (MPA; 150 cm/s), descending aorta (DAo; 150 cm/s), superior vena cava (SVC; 100 cm/s), ductus arteriosus (DA; 150 cm/s), left and right pulmonary arteries (LPA/RPA; 80 cm/s), left and right carotid arteries (CCA; 100 cm/s), umbilical vein (UV; 50 cm/s) and ductus venosus (DV; 100 cm/s) using the following parameters: flip angle: 30°; repetition time (TR): 5.6 ms; echo time (TE): 3.18 ms; field of view (FOV): 240 mm; in-plane resolution: $1.0 \times 1.0\,mm^2$; slice thickness: 5.0 mm (i.e., voxel size: 1.0 × 1.0 × 5.0); number of signal averages: 3; views per segment: 2; acceleration factor: 2, according to our previously published technique (31, 40, 55). With 15 acquired phases in the cardiac cycle, these parameters achieve a temporal resolution of ~28 ms. The typical acquisition time for each vessel was ~2–3 min. PC cine images were acquired in the short axis plane of the vessels of interest, which were prescribed using two perpendicular long axis views of each vessel. Pulmonary blood flow (PBF) was determined as the sum of blood flow in the LPA and RPA. Right ventricular cardiac output (RVCO) was determined as the sum of DA and PBF. Left ventricular cardiac output (LVCO) was determined as equal to AAo blood flow and did not include coronary blood flow. Combined ventricular output was determined as sum of RVCO and LVCO. During the normoxia state, blood flow was measured in the uterine arteries as previously described (7, 51).

2.6 Determination of oxygen saturation within the fetal circulation

Due to the paramagnetic properties of deoxyhaemoglobin, the T_2 relaxation time of blood is related to the oxygen saturation of blood (56). Vessel T_2 oximetry was performed using a T_2-prepared pulse sequence with a balanced steady-state free precession acquisition (Myomaps, Siemens) (20, 44, 54, 57). MRI acquisition parameters over all subjects and vessels were: in-plane resolution: 1.3 × 1.3 mm; slice thickness: 6 mm; TR: 4.2 ms, TE: 2.1 ms, FOV: 350 mm, acceleration factor: 2, flip angle: 70°, T2 preparation times: 32, 64, 96, 128, 160, 192 ms, and acquisition time: ~50–60 s. A non-rigid motion correction algorithm was applied to compensate for slight in-plane fetal movement (co-registration) (58).

The T_2 relaxation time for each vessel of interest was analysed using a custom lab-developed software written in Python (https://github.com/shportnoy/blood_roi_tool). The regions-of-interest were manually adjusted for each image slice to cover the central 60% of the vessel of interest (UV, DV, AAo, MPA, DA, DAo & SVC) (34, 59). Oxygen saturation was then calculated from T_2 relaxation time using the T_2-oxygen saturation relationship for sheep blood as previously described (54).

2.7 Determination of oxygen delivery and consumption

Blood flow and T_2 derived oxygen saturations were combined to calculate overall fetal DO_2, fetal VO_2, cerebral DO_2, cerebral VO_2 and pulmonary DO_2 using the following equations:

(1) Fetal DO_2:

$$DO_2 = 1.36 \times [Hb] \times Y_{UV} \times Q_{UV}$$

(2) Cerebral DO_2:

$$DO_2 = 1.36 \times [Hb] \times Y_{AAo} \times Q_{CCa}$$

(3) Fetal VO_2:

$$VO_2 = 1.36 \times [Hb] \times (Y_{UV} - Y_{DAo}) \times Q_{UV}$$

(4) Cerebral VO_2:

$$VO_2 = 1.36 \times [Hb] \times (Y_{AAo} - Y_{SVC}) \times Q_{CCa}$$

where Q_{UV} represents the measured umbilical vein blood flow; Q_{CCa} represents the combined blood flow of the left and right carotid arteries; [Hb] represents the mean fetal haemoglobin concentration during MRI scan measured using fetal arterial blood sampling and conventional blood gas analysis; 1.36 is the amount of oxygen (mL at 1 atmosphere) bound per gram of haemoglobin; Y_{UV} represents the oxygen saturation of UV blood; Y_{DAo} represents the oxygen saturation of the DAo blood, Y_{AAo} represents the oxygen saturation of AAo blood and Y_{SVC} represents the oxygen saturation of the SVC.

2.8 Determination of fetal and brain weight from MRI volumetry

A three-dimensional steady-state free procession of the uterus (T_E = 1.45 ms; repetition time (TR) = 3.38 ms; flip angle: 35 deg; in-plane resolution: 1.5 × 1.5 mm; slice thickness = 2 mm; number of slices = 100–120; number of averages = 1; base resolution: 272; FOV = 400 mm; average acquisition time 4–5 min) was acquired and segmented using ITK-SNAP (version 3.8 (60)) to measure fetal and brain volumes (39). Fetal and brain volumes were used to estimate fetal and brain weights using previously described tissue specific conversion factors (61, 62).

2.9 Blood sampling and fetal blood gas measurements

After fetal surgery, fetal arterial blood samples were collected daily to monitor fetal health by measuring the partial pressure of oxygen (PaO_2), partial pressure of carbon dioxide ($PaCO_2$), oxygen saturation (SaO_2), pH, haemoglobin, haematocrit, base excess and lactate, temperature corrected to 39°C for sheep blood with a RAPIDPOINT 500 (Siemens Healthineers, Erlangen, Germany). During the MRI scan, arterial samples (0.5 mL) for fetal blood gas analysis were taken at the beginning and end of each state (normoxia and acute hypoxia).

2.10 Statistical analysis

Data were determined to be normally distributed using the Shapiro–Wilk test for normality. To determine the impact of fetal group (control vs. FGR), oxygenation state (normoxia vs. acute hypoxia) and their interaction, data were analysed by a repeated measures two-way ANOVA with a Bonferroni correction for multiple comparisons (GraphPad Prism version 8 for Windows, GraphPad Software, La Jolla California United States). Data are presented as mean ± SD and a probability of 5% ($p < 0.05$) was considered significant for all analyses.

3 Results

3.1 Uterine artery blood flow and fetal characteristics

Uterine artery blood flow was significantly lower in pregnant ewes carrying a growth restricted fetus (Figure 1A). The FGR group had significantly lower fetal volume than controls (Figures 1B,D) and when converted to weight, this also translated to the FGR group being significantly smaller than appropriately grown controls (Figure 1E). Fetal brain weight was similar between groups (Figure 1C); however, the FGR group had an increased relative brain weight when normalised to body weight (Figure 1F).

Prior to MRI and during the normoxia MRI acquisition state, growth restricted fetuses had significantly lower PaO_2 and SaO_2 than controls (Table 1). PaO_2 and SaO_2 were significantly lower during the hypoxia state than both the normoxia state and prior to MRI in both groups. There was no difference in PaO_2 and SaO_2 between FGR and controls during the hypoxia state, indicating that similar levels of fetal hypoxaemia were achieved. pH was not different between groups prior to MRI or during either normoxia or hypoxia states. pH was significantly lower in both fetal groups during the normoxia and hypoxia states in comparison to before MRI. Lactate was not different between fetal groups prior to MRI, during normoxia or hypoxia states. Lactate was higher in both fetal groups in comparison to before the MRI in the normoxia state and lactate was significantly higher during the hypoxia state in comparison to the normoxia state (Table 1). Hb and Hct were not different between control and FGR groups but were lower during both MRI states in comparison to before MRI. $PaCO_2$ was not different between fetal groups and did not change during either MRI state in comparison to before the MRI (Table 1).

3.2 Impact of acute hypoxia and FGR on fetal blood pressure and heart rate

There was no significant difference in heart rate, SBP, DBP or MAP between control and FGR groups during the MRI (Table 2).

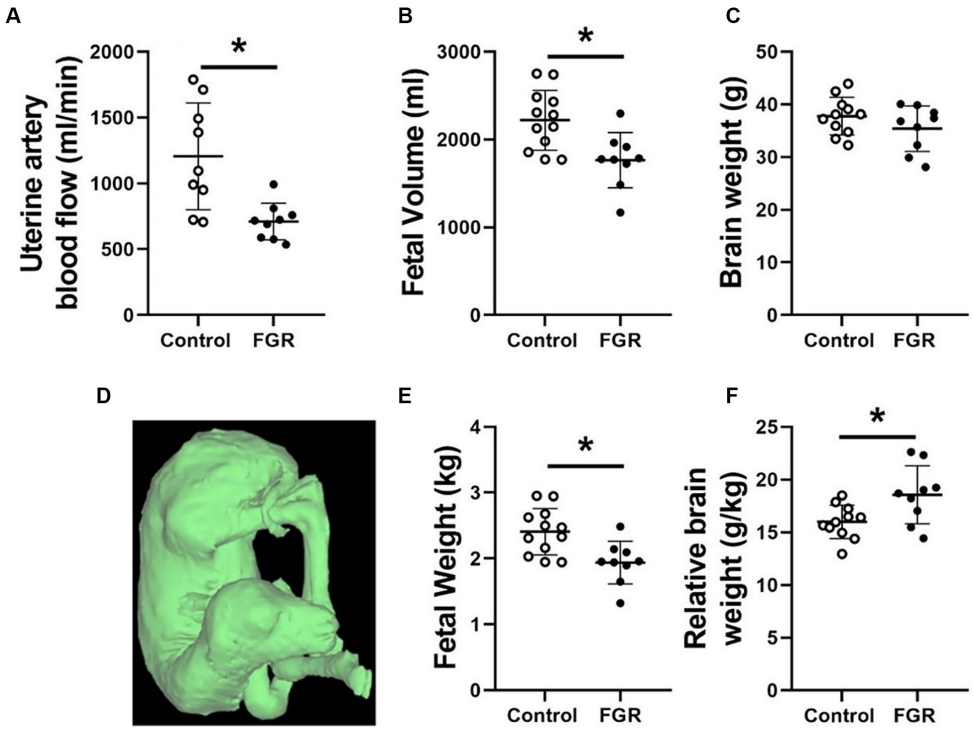

FIGURE 1
Maternal uterine artery blood flow **(A)**, fetal volume **(B)**, calculated brain weight **(C)**, representative fetal volume segmentation **(D)**, calculated fetal weight **(E)** and brain weight relative to fetal weight **(F)** in normally grown control (unfilled circles) and FGR (filled circles) fetuses. Data are presented as individual data points with mean ± SD superimposed. Data analysed using a student's unpaired *t*-test. *Statistically significant difference between groups. $p < 0.05$.

TABLE 1 Mean gestational fetal blood gas, Hb and lactate values.

	Morning of MRI		Normoxia		Hypoxia		*p*-values		
	Control ($n = 12$)	FGR ($n = 9$)	Control ($n = 12$)	FGR ($n = 9$)	Control ($n = 12$)	FGR ($n = 9$)	Group	State	Group × state
Maternal parameters									
Maternal SPO_2 (%)	—	—	97 ± 2	95 ± 5	87 ± 4[¥]	88 ± 6[¥]	0.7249	**<0.0001**	**0.0180**
Maternal heart rate (bpm)	—	—	92 ± 12	90 ± 6	97 ± 12	91 ± 7	0.4108	0.1966	0.2963
Fetal arterial parameters									
PaO_2 (mmHg)	19.9 ± 2	16.3 ± 2.4*	20.6 ± 1.8	16.2 ± 2.9 *	12.6 ± 2.5[#¥]	12.1 ± 1.7[#¥]	**0.0015**	**<0.0001**	**0.0079**
$PaCo_2$ (mmHg)	49.7 ± 4.3	51.6 ± 7.7	55.5 ± 11.6	57.3 ± 6.3	50.7 ± 12.1	55.6 ± 7.2	0.4046	0.0551	0.7054
pH	7.337 ± 0.023	7.372 ± 0.028	7.270 ± 0.050[#]	7.277 ± 0.030[#]	7.273 ± 0.053[#]	7.277 ± 0.041[#]	0.8979	**<0.0001**	0.7272
SaO_2 (%)	62.6 ± 5.8	49.2 ± 8.1*	58.5 ± 7.5	47.4 ± 7.3*	29 ± 7.6[#¥]	27.4 ± 6.1[#¥]	**0.0024**	**<0.0001**	*0.0525*
Hb (g/L)	128 ± 15	127 ± 13	98 ± 9[#]	92 ± 10[#]	98 ± 11[#]	100 ± 10[#]	0.2556	**<0.0001**	0.2561
Hct (%)	37 ± 5	36 ± 4	29 ± 3	25 ± 4	29 ± 3	27 ± 4	0.0923	**<0.0001**	0.2728
Lactate (mmol/L)	1.28 ± 0.33	1.32 ± 0.18	2.68 ± 1.37[#]	2.75 ± 1.32[#]	3.54 ± 1.68[#]	3.81 ± 1.80[#¥]	0.9827	**<0.0001**	0.6645

Values are mean ± SD. Data analysed by a repeated measures two-way ANOVA with Bonferroni's correction for multiple comparisons. [#]Significantly different to conscious state. [¥]Significantly different to normoxia state. *Significantly different between control and FGR groups within a given state. Bolded italic values are those values that represent statistical significance ($p < 0.05$).

TABLE 2 Fetal heart rate and blood pressure during MRI in normoxia and acute hypoxia states.

	Normoxia		Acute hypoxia		*p*-values		
	Control (n = 12)	FGR (n = 9)	Control (n = 12)	FGR (n = 9)	Group	State	Group × state
Heart Rate (bpm)	140 ± 10	142 ± 16	146 ± 21	148 ± 19	0.3869	0.3090	0.3438
SBP (mmHg)	42 ± 5	44 ± 9	45 ± 6	45 ± 8	0.8513	0.1684	0.6201
DBP (mmHg)	27 ± 4	27 ± 5	29 ± 6	28 ± 7	0.0733	1.2680	0.9384
MAP (mmHg)	35 ± 7	34 ± 6	37 ± 9	34 ± 5	0.5419	0.1070	0.1446

Values are means ± SD. Data analysed by a repeated measures two-way ANOVA with a Bonferroni correction for multiple comparisons. *Significant difference between control and FGR groups ($p < 0.05$). #Significantly different to conscious state. ¥Significantly different to normoxia state. SBP, systolic blood pressure; DBP, diastolic blood pressure; MAP, mean arterial pressure.

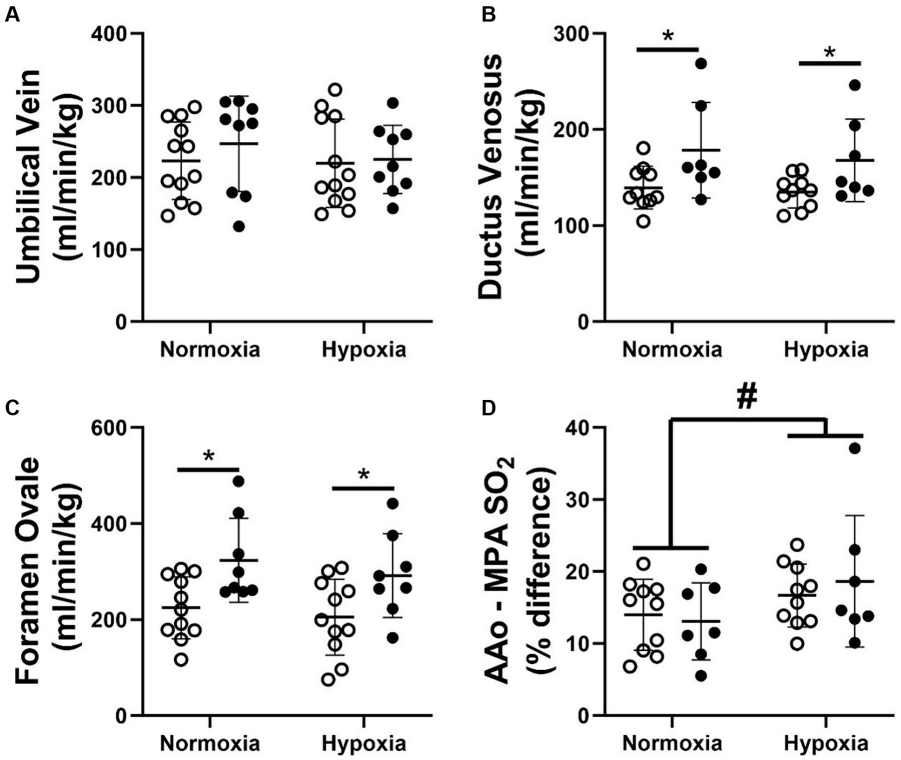

FIGURE 2
Blood flow through the umbilical vein **(A)**, ductus venosus **(B)**, foramen ovale **(C)** and the difference in blood oxygen saturation between the left and right ventricles **(D)** of normally grown control (unfilled circles) and FGR (filled circles) fetuses during nomoxia and hypoxia states. Data are presented as individual data points with mean ± SD superimposed. Data analysed by a repeated measures two-way ANOVA with a Bonferroni correction. *Statistically significant difference between groups. #Significant difference between normoxia and hypoxia states. $p < 0.05$.

Heart rate, SBP, DBP and MAP were not significantly different between normoxia and acute hypoxia MRI acquisition states (Table 2).

3.3 Impact of FGR and acute hypoxia on UV, DV and FO blood flow

There was no impact of FGR or acute hypoxia on blood flow through the UV (Figure 2A). However, blood flow through the DV and FO was significantly increased due to FGR during both the normoxia and acute hypoxia oxygenation states (Figures 2B,C, respectively). Despite being chronically hypoxaemic, FGR fetuses exhibited a similar blood SO_2 difference between the AAo and the MPA (Figure 2D). This blood SO_2 difference increased in magnitude in both control and FGR fetuses during the acute hypoxia state.

3.4 Impact of FGR and acute hypoxia on blood flow within the fetal circulation

There was no impact of FGR or oxygenation state on RVCO (Figure 3A). FGR decreased pulmonary blood flow (PBF) in comparison to normally grown control fetuses under normoxic conditions. However, there was no difference in PBF between normally grown control and FGR fetuses during acute hypoxia (Figure 3C). The blood flow passing through the DA was not

impacted by either FGR or acute hypoxia (Figure 3D). Neither FGR nor oxygenation status had an impact on LVCO (Figure 3B) or the blood flowing toward the brain via the carotid arteries (Figure 3E). There was no impact of FGR or oxygenation state on the blood flow through the superior vena cava (Figure 3F), descending aorta (Figure 3G) or the blood flowing toward the lower trunk of the fetus (Figure 3H).

There was no impact of FGR or acute hypoxia on combined ventricular output (CVO; Figure 4A). Blood flow distribution as a % of CVO was altered such that there was an increased proportion of blood flow through the FO in FGR fetuses during both the normoxia and acute hypoxia states. Blood flow distribution toward the brain through the carotid arteries (CCa) was higher in FGR than control fetuses during the normoxia state but not different during the acute hypoxia state (Figure 4B). Diagrammatic representations of oxygen transport throughout the fetal circulation in control and FGR fetuses during normoxia and acute hypoxia states are shown in Figure 5.

3.5 Impact of FGR and acute hypoxia on DO_2 and VO_2

Absolute fetal DO_2 (Figure 6A) and VO_2 (Figure 6D) of growth restricted fetuses were significantly lower than normally grown control fetuses in both normoxia and hypoxia states. Absolute fetal DO_2 and VO_2 of both FGR and control fetuses were significantly lower in the hypoxia state in comparison to the normoxia state. When normalised to fetal weight, fetal DO_2 and VO_2 were similar between control and FGR fetuses during both nomoxia and hypoxia states but significantly decreased in both groups during the hypoxia state (Figures 6B,E). There was no impact of FGR or oxygenation state on overall fetal oxygen extraction fraction (Figure 6C). FGR did not impact absolute or normalised cerebral DO_2 and VO_2. In line with the decreased fetal DO_2 during the hypoxia state, both absolute (Figure 6F) and normalised (Figure 6G) cerebral DO_2 in both normally grown and FGR fetuses was significantly decreased. Both normally grown and growth restricted fetuses had a significant

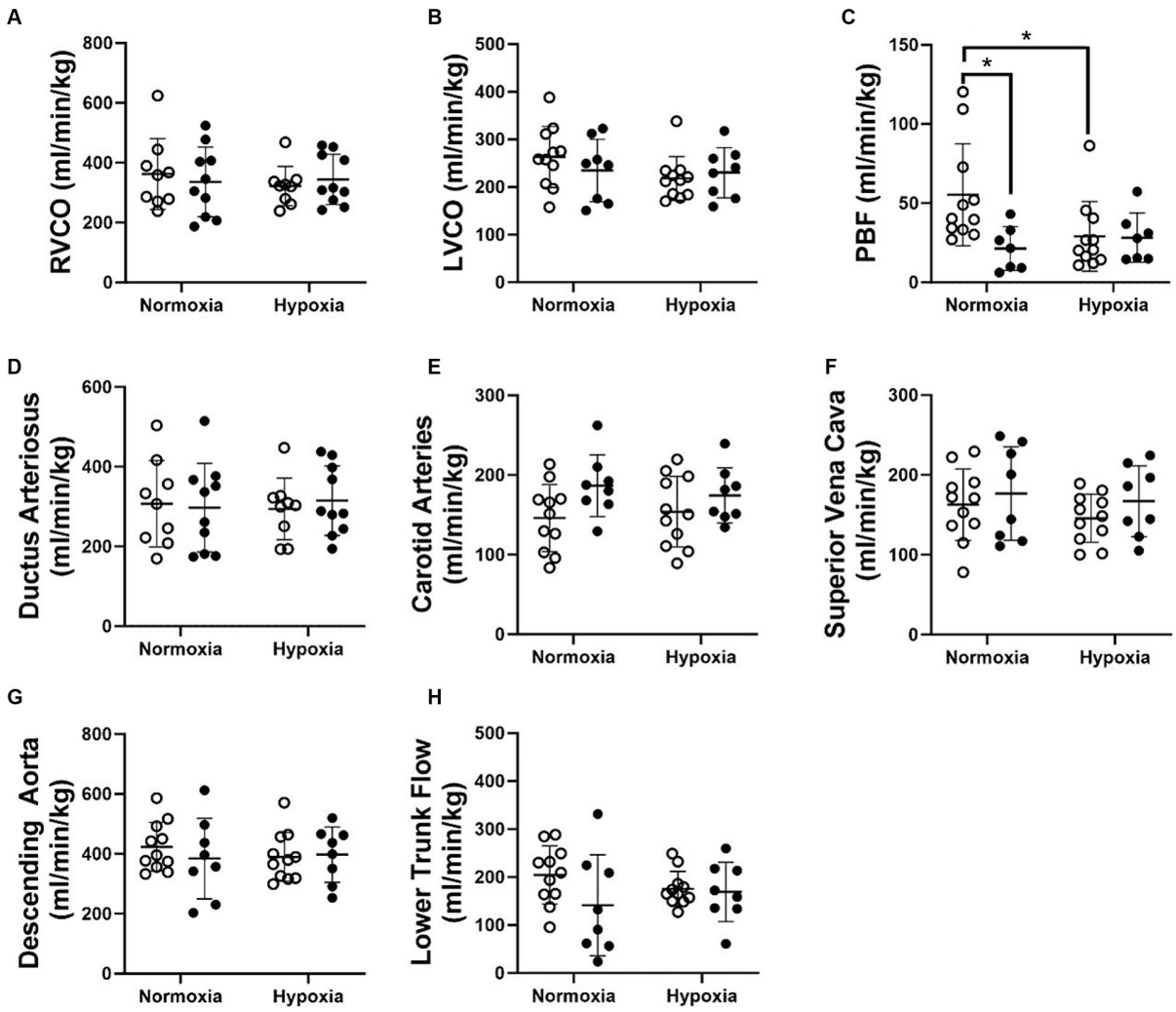

FIGURE 3
RVCO **(A)**, LVCO **(B)**, PBF **(C)** as well as blood flow through the ductus arteriosus **(D)**, carotid arteries **(E)**, superior vena cava **(F)**, descending aorta **(G)** and towards the lower trunk **(H)** in normally grown control (unfilled circles) and FGR (filled circles) fetuses. Data are presented as individual data points with mean ± SD superimposed. Data analysed using a repeated measures two-way ANOVA with a Bonferroni correction. *Statistically significant difference between groups. $p < 0.05$.

increase in cerebral oxygen extraction fraction (Figure 6H) during the hypoxia state and an unchanged absolute (Figure 6I) and normalised (Figure 6J) cerebral VO_2 compared to the normoxia state.

4 Discussion

In this study, we aimed to comprehensively characterize and differentiate the haemodynamic responses occurring during acute and chronic periods of fetal hypoxaemia. Fetal hypoxaemia may present as either an acute event or a chronic condition, both of which are associated with poor short-term outcomes during fetal life, such as FGR and stillbirth. These conditions can also result in impaired fetal development and developmental programming, leading to an increased risk of complications during the neonatal period and long-term morbidity across the individual's life course. The ability to distinguish between these two scenarios and understanding their impact on fetal haemodynamics is required for development of appropriate diagnostic tools and intervention strategies. Herein, we employed a well-established pregnant sheep model of early onset placental insufficiency (19, 63, 64), alongside clinically relevant advanced MRI techniques (31, 43, 54, 65, 66), enabling exploration of the intricate relationship between fetal haemodynamics and acute versus chronic fetal hypoxaemia.

Pregnant ewes in the FGR group of this study had significantly lower uterine artery blood flow than ewes in the control group. Thus, in combination with poor placental function, this translated to chronic fetal hypoxaemia as evidenced by significantly lower PaO_2 and SaO_2 levels in FGR compared to normally grown fetuses. Importantly, these fetuses were already smaller than the normally grown fetuses of the control group at the time of MRI assessment, with an increased brain to body weight ratio, indicating that haemodynamic adaptations associated with "brain sparing" physiology were already in place (15, 19, 21, 67, 68). It is well established that blood flow and oxygen delivery throughout the fetal circulation are sensitive to the prevailing oxygen availability (15). As such, to best recapitulate each fetuses' normal circulation prior to maternal ventilation, the level of maternal inspired oxygen during the normoxic MRI state was titrated on a case-by-case basis to match fetal blood gas status to that during the conscious state prior to the MRI. This approach resulted in lower PaO_2 and SaO_2 in FGR fetuses and is consistent with the measurement of reduced fetal DO_2 and VO_2 as determined by MRI. However, it should be noted that when fetal DO_2 and VO_2 were normalized to fetal weight, the significant difference in these measures between the control and growth-restricted fetuses was mitigated. This is in contrast to ultrasound and MRI based studies in humans, which found the significant reduction in fetal DO_2 within the FGR group is maintained after the normalization for fetal weight (20, 69). This may be explained either by a species specific aspect or differences in the timing, duration and severity of the growth restriction induced in the present study compared to the aforementioned human studies that focused on late-onset FGR (14, 20, 68).

Similar to the MRI based study in late-onset human FGR cases by Zhu et al. (20), we comprehensively characterised the impact of chronic hypoxaemia on the major vessels within the fetal circulation in a model of early-onset FGR. Uniquely, the fetal circulation incorporates specialised shunts: the foramen ovale and ductus arteriosus, that enable blood to bypass the fetal lungs (70). An additional fetal shunt, the DV, redirects a portion of the well oxygenated umbilical venous return away from the liver and toward the posterior side of the inferior vena cava where it is preferentially streamed toward the foramen ovale and shunted from the right to the left side of the heart (52, 54, 71, 72). In the present study, we found that chronically hypoxaemic FGR fetuses had increased blood flow through the DV. This finding builds on our previous work using MRI to characterise the fetal circulation of late-onset growth restricted human fetuses, where we did not measure blood flow through the DV (20), and is consistent with the seminal ultrasound based studies evaluating the umbilical circulation in FGR human fetuses with and without abnormal umbilical artery (UA) pulsatility index (73–75). This study adds to our knowledge of the fetal circulation in the setting of growth restriction by showing that, in addition to increased DV flow, right to left heart shunting through the FO was increased with a corresponding decrease in PBF. Given that left ventricular preload blood pool is comprised of both oxygen-rich blood being shunted through the FO from the right side of the heart and pulmonary venous return, this finding suggests that the composition of the left ventricular preload blood pool in FGR fetuses is shifted to include a greater proportion of oxygen-rich blood from the DV-FO pathway. Utilising T_2 oximetry, we confirmed this notion, and show that despite the FGR

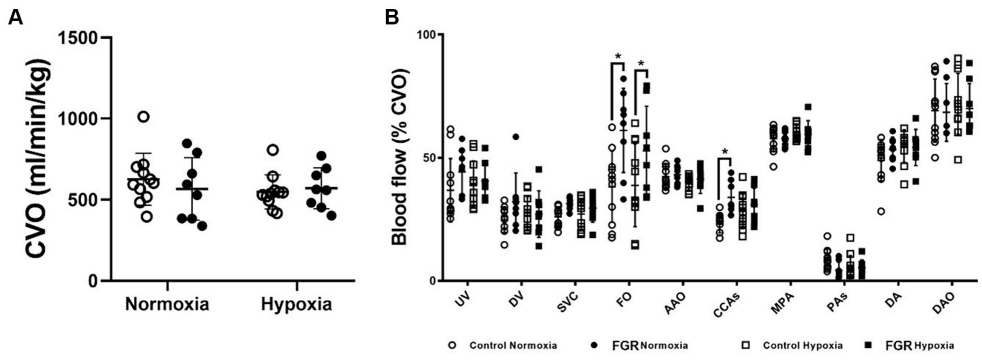

FIGURE 4
Effect of FGR and acute hypoxia on combined ventricular output (CVO; **A**) and blood flow distribution as a percentage of CVO within the fetal circulation **(B)**. Data are presented as individual data points with mean ± SD superimposed. Data analysed using a repeated measures two-way ANOVA with a Bonferroni correction. *Statistically significant difference between groups. $p < 0.05$.

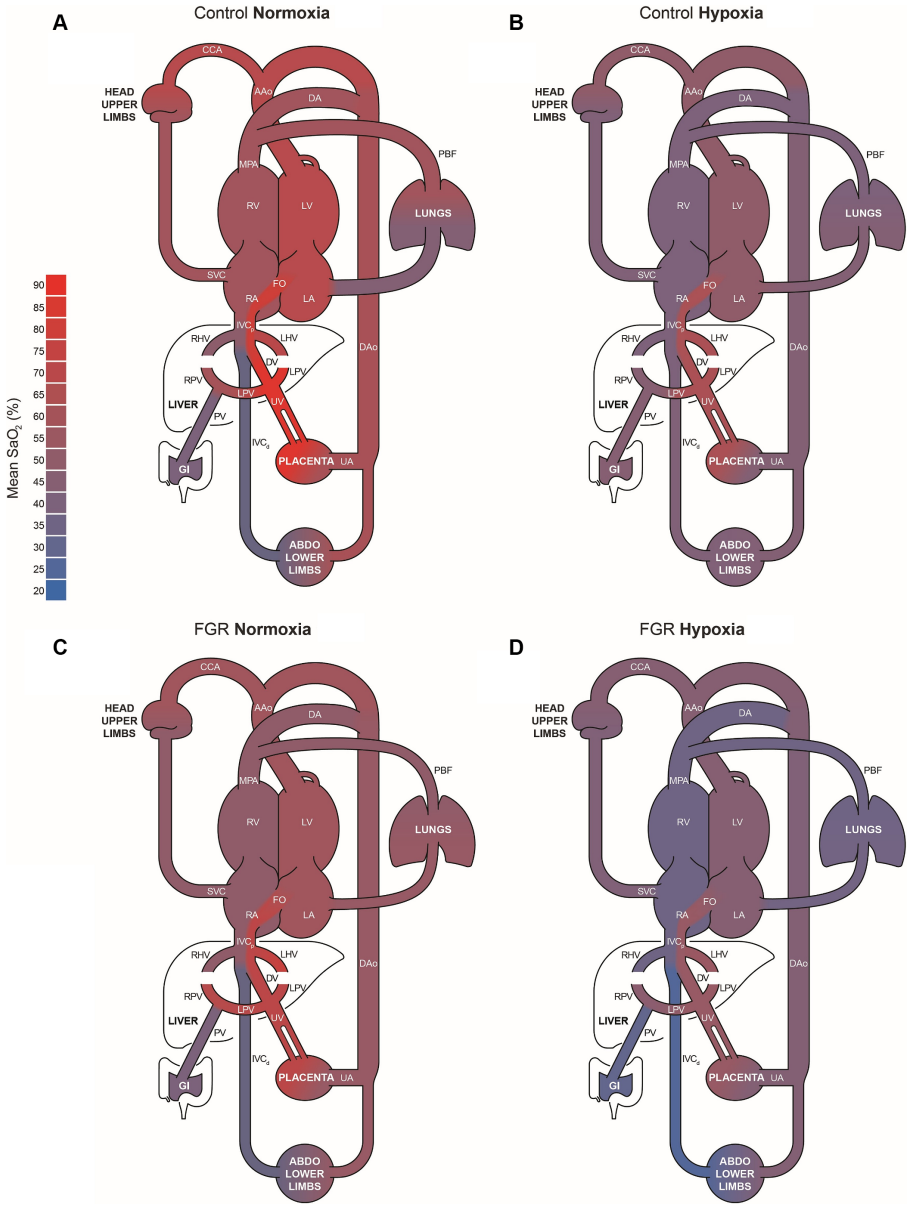

FIGURE 5
Colour coded diagrammatic representations of oxygen transport throughout the fetal circulation in control **(A, B)** and FGR **(C, D)** fetuses during normoxia and hypoxia states. Differences in the width of each vessel indicate where there are significant differences in blood flow between states and across groups. AAo, ascending aorta; CCA, combined carotid arteries; DA, ductus arteriosus; DAo, descending aorta; DV, ductus venosus; FO, foramen ovale; IVC, inferior vena cava; LA, left atrium; LHV, left hepatic vein; LV, left ventricle; MPA, main pulmonary artery; PBF, pulmonary blood flow; PV, portal vein; RA, right atrium; RV, right ventricle; RHV, right hepatic vein; SVC, superior vena cava; UA, umbilical artery; UV, umbilical vein.

fetuses in the present study being systemically hypoxaemic, the percent difference in SaO_2 between the blood in ascending aorta flowing towards the brain and the blood in the MPA was similar between chronically hypoxaemic FGR and control fetuses. Although this is beneficial for the brain *in utero*, the alterations in both hepatic and pulmonary haemodynamics required to aid in and ensure this process may be to the detriment of the liver and lungs, respectively. The increased DV shunting and thus reduced liver perfusion of well oxygenated and glucose rich blood returning from the placenta may contribute towards impaired liver growth in hypoxaemic growth restricted fetuses (76), a factor that is associated with reduced concentrations of key fetal growth factors, insulin-like growth factor (IGF)-1 and IGF-2 (77), and may predispose FGR born offspring to metabolic syndrome and impaired drug metabolism across the life course (67, 78–82). Moreover, hypoxaemia driven increases in pulmonary vascular resistance, and thus reduced PBF and DO_2, may be the mechanism by which growth restricted fetuses exhibit delayed surfactant maturation (83, 84) and increased rates of persistent pulmonary hypertension (85).

Interestingly, and contrary to studies investigating haemodynamic changes during acute fetal hypoxemia that typically exhibit increased blood flow towards the brain (15, 86, 87), we found no significant difference in absolute carotid artery blood flow between control and FGR groups. Similar findings have been shown in human (20) and

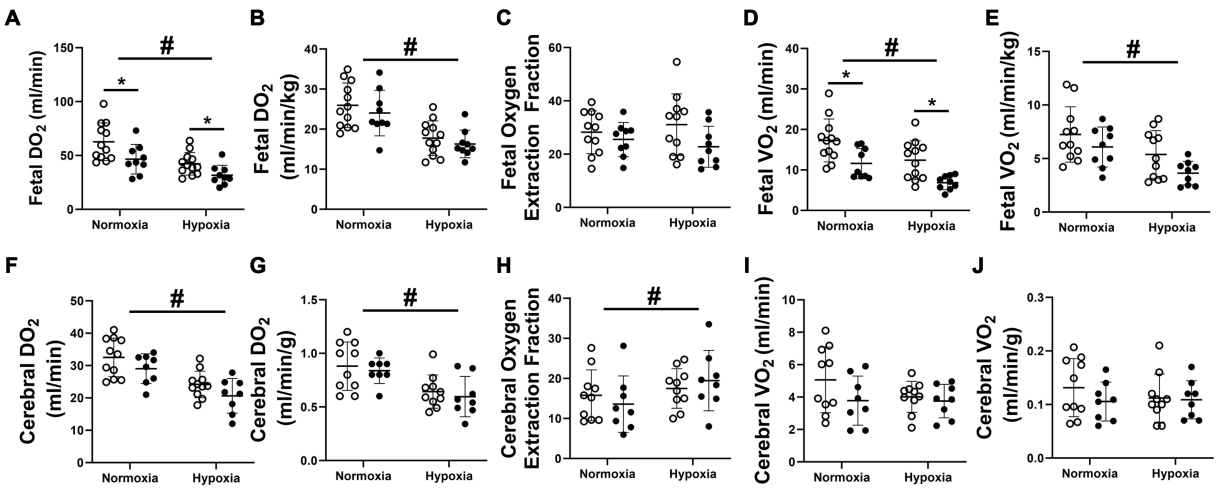

FIGURE 6
Fetal absolute **(A)** and normalised **(B)** DO_2, oxygen extraction fraction **(C)** and absolute **(D)** and normalised **(E)** VO_2 as well as absolute **(F)** and normalised **(G)** cerebral DO_2, cerebral oxygen extraction fraction **(H)** and absolute **(I)** and normalised **(J)** cerebral VO_2 in normally grown control (unfilled circles) and FGR (filled circles) fetuses. Data are presented as individual data points with mean ± SD superimposed. Data analysed by a repeated measures two-way ANOVA with a Bonferroni correction. *Significant difference between normally grown and growth restricted fetuses. #Statistically significant difference between oxygen states. $p < 0.05$.

sheep (19, 21) studies of FGR, whereby either more than a third or the entirety of FGR fetuses studied exhibited normal cerebral blood flow. However, it should be noted that when assessed as a proportion of CVO, blood flow toward the brain was increased in FGR fetuses during the normoxic MRI acquisition state but not different to normally grown controls during the acute hypoxia state. Despite the prevailing level of fetal hypoxemia, cerebral DO_2 in the FGR group remained similar to controls, supporting the presence of an alternative "brain sparing" mechanism in chronically hypoxaemic FGR fetuses. Thus, a preferential streaming of oxygen rich blood via the DV-FO pathway may work in tandem with an attempt to redistribute blood flow toward the brain. The identification and characterisation of this mechanism in this well-established preclinical model of FGR may allow for better diagnosis of at risk FGR fetuses without abnormal UA pulsatility indexes by using MRI analysis of blood flow and oximetry in the fetal circulation.

Chronically hypoxaemic FGR fetuses are just as likely to experience acute hypoxaemic episodes as normally grown fetuses (e.g., acute transient cord occlusions). However, this is harder to model in a preclinical setting and is therefore less well studied. Thus, the second layer of this study was to determine whether acute-on-chronic hypoxaemia induced unique haemodynamic patterns to maintain oxygen delivery to critical tissues whilst still accommodating for the challenges posed by prolonged oxygen restriction. Previously, different conclusions on this matter have been reported with either a maintenance of the acute hypoxaemia induced cardiac output redistribution in chronically hypoxaemic fetuses (22, 23, 88, 89), a sensitization of the cardiovascular response to acute hypoxaemia (22, 23) or even a blunting of this response (90, 91). However, it should be noted that these studies focussed on the immediate (within 5 min) fetal cardiovascular response to acute hypoxia, whereas the present study aimed to characterize the haemodynamic profile of fetuses after the initial response; at which point acute hypoxaemia was established (over an hour). During the acute hypoxaemia state, both normally grown control and chronically hypoxaemic FGR fetuses reached similar levels of hypoxaemia as measured by both conventional blood gas analysis and by MRI derived fetal DO_2. It could be argued that a limitation of the present study may be that, due to the prevailing extent of hypoxaemia in the FGR group, the magnitude of the drop in fetal oxygenation was higher in normally grown control fetuses. Although changes in fetal PaO_2 are detected by the carotid bodies, the concept of a fixed "set point" for hypoxaemia detection by these carotid bodies and the consequent activation of a haemodynamic response is not yet fully established. The PaO_2 achieved during the acute hypoxaemia MRI acquisition state are in line with previous studies investigating the haemodynamic responses to acute hypoxaemia in fetal sheep (86, 92). Much like advancing gestation, prior exposure to hypoxaemia may alter carotid body sensitivity and the subsequent initiation of a haemodynamic response. Therefore, different severities of decreased PaO_2 may elicit varying responses, rather than the response being based on passing a fixed "set point." Indeed, previous work has shown that the chronically hypoxaemic fetus regards the hypoxaemia that it operates under as normal with no changes in carotid body signaling that are seen in response to acute hypoxia (93). Although we have previously shown the chronically hypoxaemic fetus to have a greater reliance on α-adrenergic stimuli to regulate its blood pressure (94), comparative studies assessing the blood pressure responses in the presence of either a post-ganglionic or an α-adrenergic antagonist indicate that the increased reliance on α-adrenergic stimuli is due to hyperinnervation of the peripheral vasculature that is driven by hypoxaemia (95, 96). However, this hyperinnervation is not present at the gestational ages assessed in present study but rather develops as gestation progresses becoming apparent 2 weeks later at ~130 days gestation. Reducing fetal PaO_2 to a comparable degree in control and FGR fetuses has allowed the present study to disentangle any influence that prior and prevailing chronic hypoxaemia may have on the haemodynamic response. Overall, both control and FGR fetuses exhibited similar reductions in fetal VO_2, a well-known fetal response to acute hypoxia often linked to reduced fetal breathing movements (97), reduced hind limb VO_2

(98) and a general shift away from processes that may require more oxygen (15, 92).

Whilst the increased flow through the DV-FO pathway in the FGR group was maintained during the second hit of acute hypoxaemia and the blood SO_2 percent difference between the ascending aorta and the main pulmonary artery higher than during the normoxia state, this increased right to left heart shunting was unable to maintain cerebral DO_2. Indeed, cerebral DO_2 in both groups was significantly lower during the acute hypoxaemia state and FGR fetuses responded identically to control fetuses, by increasing cerebral oxygen extraction fraction to maintain cerebral VO_2. An interesting finding was the lack of change in DV blood flow in control fetuses in response to acute hypoxaemia. Previously, it has generally been considered that in response to acute hypoxaemia, blood flow through the DV increases (99–102) with evidence that this may be due to a hypoxaemia driven α—adrenergic vasoconstriction within the liver, and thus, an increased hepatic vascular resistance allowing more blood to bypass the liver in favour of the DV (102). Thus, a possible explanation of our contrasting results concerning blood flow through the DV may be the extent of α-adrenergic innervation of vascular tone within the fetal liver at the time of the study. The reliance that the fetus has for blood pressure regulation through α-adrenergic innervation of the vasculature not only increases with chronic hypoxaemia but also with advancing gestational age (95). Although previous studies investigated the impact of acute hypoxaemia on DV flow across a range of gestational ages, to the best of our knowledge, the present study was performed at the youngest gestational age to date, and thus, this regulatory mechanism may not have been mature enough to illicit a measurable change in blood flow through the DV. Alternatively, it is possible that DV is directly rather than indirectly innervated by α-adrenergic mechanisms and that such direct innervation of the DV is not yet mature in the fetal sheep of the present study. Previously, *ex vivo* studies into the DV of late gestation fetal sheep found them to not only contain adrenergic fibres but also to respond increasingly to α-adrenergic stimuli as gestational age advanced and oxygen tension increased (103). This suggests a key interplay between the prevailing oxygen tension and gestational age in the regulation of DV tone. Indeed, placental insufficiency induced reduction in oxygen content of the blood within the UV may have altered the tone of the DV of the FGR sheep of the present study and explain the increased DV flow. Gestational age of the fetuses of the present study may also explain why we did not observe a decrease in PBF in response to acute hypoxia. Previous studies in fetal sheep have shown that the pulmonary response to hypoxaemia was not developed at 112–119 days GA (present study ~118 days GA), and that the increase in pulmonary vascular resistance and decreased pulmonary blood flow in response to acute hypoxia was only observed from 121 days GA onwards due to a progressive increase in pulmonary vasomotor tone across gestation (104). Nonetheless, we have shown that at this gestational age, increased DV-FO streaming is present in response to chronic hypoxaemia, but not yet a present adaptation in response to acute hypoxaemia.

The present study has several limitations related to the model of FGR and with the need for anaesthesia during the MRI acquisition. Herein, we utilised the well-established carunclectomy model of early onset placental insufficiency and FGR. Whilst, this model results in chronic fetal hypoxaemia, it should be noted that this is not in isolation from reductions in the supply of other substrates or hormones to the fetus (68, 94, 105, 106). As such, there is the possibility that the reductions in other metabolic substrates and/or hormones may also play a role in the fetal haemodynamic response. Although our previous work comparing the fetal haemodynamic response to acute hypoxaemia in the presence of different anaesthetic regimens found isoflurane to be the most appropriate anaesthetic agent (107); there are still caveats that need to be noted in order to fully understand our findings. The immediate haemodynamic response to acute hypoxaemia includes an initial bradycardia followed by a rise in MAP (15). However, whilst under the influence of isoflurane, there is no bradycardia but rather a short-lived tachycardia (107). Whilst our MRI acquisitions of fetal blood flow and oximetry were performed after this initial response to acute hypoxaemia had subsided and fetal heart rate was not different to the normoxia state, the flows reported may not represent the same physiological response to acute hypoxaemia as may have occurred without the presence of anaesthesia. Furthermore, isoflurane has been linked to cerebral vasodilation as well as a reduction in cerebral metabolism (108). As such, it is possible that carotid blood flow may have already been elevated above true baseline levels in the normoxia state—even before acute hypoxaemia, and thus, a significant difference in carotid artery blood flow and cerebral DO_2 between control and FGR fetuses as well as between the normoxia and acute hypoxaemia states could have been masked.

In summary, this study has utilised a combination of clinically relevant MRI techniques and a well-established sheep model of placental insufficiency induced FGR to characterise haemodynamics of the growth restricted fetus and assess their ability to respond to a secondary episode of acute hypoxaemia. We have shown clear evidence for the importance of the preferential streaming mechanism, whereby oxygen rich blood is preferentially streamed through the DV-FO pathway to maintain cerebral DO_2. However, this preferential streaming is aided by alterations to pulmonary haemodynamics that may manifest as respiratory complications at birth (109). When challenged with an acute episode of hypoxaemia, unlike their normally grown counterparts, PBF in FGR fetuses had already reached its lower plateau, which may have impeded further increases in FO flow to deal with the worsening hypoxaemia. The present study has laid the foundation for future studies to utilise MRI to determine how the haemodynamics in FGR change as gestation progresses, isolate the gestational age at which the DV becomes responsive to acute hypoxaemia and evaluate the maturation of the response to acute-on-chronic hypoxaemia.

Data availability statement

The raw data supporting the conclusions of this article will be made available by the authors, without undue reservation.

Ethics statement

The animal study was approved by Animal Ethics Committee of the South Australian Health and Medical Research Institute (SAHMRI). The study was conducted in accordance with the local legislation and institutional requirements.

Author contributions

JRTD: Data curation, Formal analysis, Investigation, Methodology, Project administration, Software, Validation, Writing – original draft, Writing – review & editing. BSS: Data curation, Formal analysis, Investigation, Methodology, Software, Writing – review & editing. SLH: Investigation, Methodology, Project administration, Supervision, Validation, Writing – review & editing. SJH: Data curation, Formal analysis, Investigation, Software, Writing – review & editing. SRP: Data curation, Methodology, Software, Writing – review & editing. CKM: Conceptualization, Data curation, Formal analysis, Funding acquisition, Investigation, Methodology, Resources, Software, Supervision, Visualization, Writing – review & editing. MS: Conceptualization, Data curation, Formal analysis, Funding acquisition, Investigation, Methodology, Project administration, Resources, Software, Supervision, Validation, Visualization, Writing – review & editing. JLM: Conceptualization, Data curation, Formal analysis, Funding acquisition, Investigation, Methodology, Project administration, Resources, Software, Supervision, Validation, Visualization, Writing – review & editing.

Funding

The author(s) declare that financial support was received for the research, authorship, and/or publication of this article. The work was funded by a grant from the Canadian Institutes of Health Research (PJT-148712) awarded to MS, JLM, and CKM. JLM was funded by an ARC Future Fellowship (Level 3; FT170100431).

Acknowledgments

The authors acknowledge the technical assistance of the National Imaging Facility, a NCRIS capability, at PIRL, SAHMRI.

Conflict of interest

The authors declare that the research was conducted in the absence of any commercial or financial relationships that could be construed as a potential conflict of interest.

The author(s) declared that they were an editorial board member of Frontiers, at the time of submission. This had no impact on the peer review process and the final decision.

Publisher's note

References

1. Colella M, Frerot A, Novais ARB, Baud O. Neonatal and long-term consequences of fetal growth restriction. *Curr Pediatr Rev*. (2018) 14:212–8. doi: 10.2174/1573396314666180712114531

2. Froen JF, Gardosi JO, Thurmann A, Francis A, Stray-Pedersen B. Restricted fetal growth in sudden intrauterine unexplained death. *Acta Obstet Gynecol Scand*. (2004) 83:801–7. doi: 10.1111/j.0001-6349.2004.00602.x

3. Gordijn SJ, Beune IM, Ganzevoort W. Building consensus and standards in fetal growth restriction studies. *Best Pract Res Clin Obstet Gynaecol*. (2018) 49:117–26. doi: 10.1016/j.bpobgyn.2018.02.002

4. Malhotra A, Allison BJ, Castillo-Melendez M, Jenkin G, Polglase GR, Miller SL. Neonatal morbidities of fetal growth restriction: pathophysiology and impact. *Front Endocrinol*. (2019) 10:55. doi: 10.3389/fendo.2019.00055

5. Barcroft J, Herkel W, Hill S. The rate of blood flow and gaseous metabolism of the uterus during pregnancy. *J Physiol*. (1933) 77:194–206. doi: 10.1113/jphysiol.1933.sp002963

6. Richardson BS, de Vrijer B, Brown HK, Stitt L, Choo S, Regnault TRH. Gestational age impacts birth to placental weight ratio and umbilical cord oxygen values with implications for the fetal oxygen margin of safety. *Early Hum Dev*. (2022) 164:105511. doi: 10.1016/j.earlhumdev.2021.105511

7. Saini BS, Darby JRT, Marini D, Portnoy S, Lock MC, Yin Soo J, et al. An MRI approach to assess placental function in healthy humans and sheep. *J Physiol*. (2021) 599:2573–602. doi: 10.1113/JP281002

8. Battaglia FC, Meschia G. Principal substrates of fetal metabolism. *Physiol Rev*. (1978) 58:499–527. doi: 10.1152/physrev.1978.58.2.499

9. Baschat AA. Fetal responses to placental insufficiency: an update. *BJOG*. (2004) 111:1031–41. doi: 10.1111/j.1471-0528.2004.00273.x

10. Figueras F, Gardosi J. Intrauterine growth restriction: new concepts in antenatal surveillance, diagnosis, and management. *Am J Obstet Gynecol*. (2011) 204:288–300. doi: 10.1016/j.ajog.2010.08.055

11. Giussani DA, Unno N, Jenkins SL, Wentworth RA, Derks JB, Collins JH, et al. Dynamics of cardiovascular responses to repeated partial umbilical cord compression in late-gestation sheep fetus. *Am J Phys*. (1997) 273:H2351–60. doi: 10.1152/ajpheart.1997.273.5.H2351

12. Turner JM, Mitchell MD, Kumar SS. The physiology of intrapartum fetal compromise at term. *Am J Obstet Gynecol*. (2020) 222:17–26. doi: 10.1016/j.ajog.2019.07.032

13. Bennet L. Sex, drugs and rock and roll: tales from preterm fetal life. *J Physiol*. (2017) 595:1865–81. doi: 10.1113/JP272999

14. Morrison JL. Sheep models of intrauterine growth restriction: fetal adaptations and consequences. *Clin Exp Pharmacol Physiol*. (2008) 35:730–43. doi: 10.1111/j.1440-1681.2008.04975.x

15. Giussani DA. The fetal brain sparing response to hypoxia: physiological mechanisms. *J Physiol*. (2016) 594:1215–30. doi: 10.1113/JP271099

16. Thornburg KL. Fetal response to intrauterine stress. *Ciba Found Symp*. (1991) 156:17–29. doi: 10.1002/9780470514047.ch3

17. Bartelds B, van Bel F, Teitel DF, Rudolph AM. Carotid, not aortic, chemoreceptors mediate the fetal cardiovascular response to acute hypoxemia in lambs. *Pediatr Res*. (1993) 34:51–5. doi: 10.1203/00006450-199307000-00013

18. Bennet L, Gunn AJ. The fetal heart rate response to hypoxia: insights from animal models. *Clin Perinatol*. (2009) 36:655–72. doi: 10.1016/j.clp.2009.06.009

19. Poudel R, McMillen IC, Dunn SL, Zhang S, Morrison JL. Impact of chronic hypoxemia on blood flow to the brain, heart, and adrenal gland in the late-gestation IUGR sheep fetus. *Am J Physiol Regul Integr Comp Physiol*. (2015) 308:R151–62. doi: 10.1152/ajpregu.00036.2014

20. Zhu MY, Milligan N, Keating S, Windrim R, Keunen J, Thakur V, et al. The hemodynamics of late-onset intrauterine growth restriction by MRI. *Am J Obstet Gynecol*. (2016) 214:367.e1–367.e17. doi: 10.1016/j.ajog.2015.10.004

21. Miller SL, Supramaniam VG, Jenkin G, Walker DW, Wallace EM. Cardiovascular responses to maternal betamethasone administration in the intrauterine growth-restricted ovine fetus. *Am J Obstet Gynecol*. (2009) 201:613.e1–8. doi: 10.1016/j.ajog.2009.07.028

22. Block BS, Llanos AJ, Creasy RK. Responses of the growth-retarded fetus to acute hypoxemia. *Am J Obstet Gynecol*. (1984) 148:878–85. doi: 10.1016/0002-9378(84)90529-5

23. Gardner DS, Fletcher AJ, Bloomfield MR, Fowden AL, Giussani DA. Effects of prevailing hypoxaemia, acidaemia or hypoglycaemia upon the cardiovascular, endocrine and metabolic responses to acute hypoxaemia in the ovine fetus. *J Physiol*. (2002) 540:351–66. doi: 10.1113/jphysiol.2001.013434

24. Gardosi J, Madurasinghe V, Williams M, Malik A, Francis A. Maternal and fetal risk factors for stillbirth: population based study. *BMJ*. (2013) 346:f108. doi: 10.1136/bmj.f108

25. Miller SL, Huppi PS, Mallard C. The consequences of fetal growth restriction on brain structure and neurodevelopmental outcome. *J Physiol*. (2016) 594:807–23. doi: 10.1113/JP271402

26. Eixarch E, Meler E, Iraola A, Illa M, Crispi F, Hernandez-Andrade E, et al. Neurodevelopmental outcome in 2-year-old infants who were small-for-gestational age term fetuses with cerebral blood flow redistribution. *Ultrasound Obstet Gynecol*. (2008) 32:894–9. doi: 10.1002/uog.6249

27. Oros D, Figueras F, Cruz-Martinez R, Padilla N, Meler E, Hernandez-Andrade E, et al. Middle versus anterior cerebral artery Doppler for the prediction of perinatal outcome and neonatal neurobehavior in term small-for-gestational-age fetuses with normal umbilical artery Doppler. *Ultrasound Obstet Gynecol*. (2010) 35:456–61. doi: 10.1002/uog.7588

28. Tolsa CB, Zimine S, Warfield SK, Freschi M, Sancho Rossignol A, Lazeyras F, et al. Early alteration of structural and functional brain development in premature infants born with intrauterine growth restriction. *Pediatr Res*. (2004) 56:132–8. doi: 10.1203/01.PDR.0000128983.54614.7E

29. Pearce W. Hypoxic regulation of the fetal cerebral circulation. *J Appl Physiol*. (2006) 100:731–8. doi: 10.1152/japplphysiol.00990.2005

30. Seed M, van Amerom JF, Yoo SJ, Al Nafisi B, Grosse-Wortmann L, Jaeggi E, et al. Feasibility of quantification of the distribution of blood flow in the normal human fetal circulation using CMR: a cross-sectional study. *J Cardiovasc Magn Reson*. (2012) 14:82. doi: 10.1186/1532-429X-14-79

31. Duan AQ, Darby JRT, Soo JY, Lock MC, Zhu MY, Flynn LV, et al. Feasibility of phase-contrast cine magnetic resonance imaging for measuring blood flow in the sheep fetus. *Am J Physiol Regul Integr Comp Physiol*. (2019) 317:R780–92. doi: 10.1152/ajpregu.00273.2017

32. Prsa M, Sun L, van Amerom J, Yoo SJ, Grosse-Wortmann L, Jaeggi E, et al. Reference ranges of blood flow in the major vessels of the normal human fetal circulation at term by phase-contrast magnetic resonance imaging. *Circ Cardiovasc Imaging*. (2014) 7:663–70. doi: 10.1161/CIRCIMAGING.113.001859

33. van Amerom JF, Goolaub DS, Schrauben EM, Sun L, Macgowan CK, Seed M. Fetal cardiovascular blood flow MRI: techniques and applications. *Br J Radiol*. (2023) 96:20211096. doi: 10.1259/bjr.20211096

34. Portnoy S, Milligan N, Seed M, Sled JG, Macgowan CK. Human umbilical cord blood relaxation times and susceptibility at 3 T. *Magn Reson Med*. (2017) 79:3194–206. doi: 10.1002/mrm.26978

35. Portnoy S, Osmond M, Zhu MY, Seed M, Sled JG, Macgowan CK. Relaxation properties of human umbilical cord blood at 1.5 Tesla. *Magn Reson Med*. (2017) 77:1678–90. doi: 10.1002/mrm.26231

36. Portnoy S, Seed M, Sled JG, Macgowan CK. Non-invasive evaluation of blood oxygen saturation and hematocrit from T1 and T2 relaxation times: *in-vitro* validation in fetal blood. *Magn Reson Med*. (2017) 78:2352–9. doi: 10.1002/mrm.26599

37. Morrison JL, Williams GK, Cho SKS, Saini BS, Meakin AS, Holman SL, et al. MRI characterization of blood flow and oxygen delivery in the fetal sheep whilst exposed to sildenafil citrate. *Neonatology*. (2022) 119:735–44. doi: 10.1159/000526972

38. Darby JRT, Schrauben EM, Saini BS, Holman SL, Perumal SR, Seed M, et al. Umbilical vein infusion of prostaglandin I_2 increases ductus venosus shunting of oxygen rich blood but does not increase cerebral oxygen delivery in the fetal sheep. *J Physiol*. (2020) 598:4957–67. doi: 10.1113/JP280019

39. Aujla T, Darby JRT, Saini BS, Lock MC, Holman SL, Bradshaw EL, et al. Impact of resveratrol-mediated increase in uterine artery blood flow on fetal haemodynamics, blood pressure and oxygenation in sheep. *Exp Physiol*. (2021) 106:1166–80. doi: 10.1113/EP089237

40. Dimasi CG, Lazniewska J, Plush SE, Saini BS, Holman SL, Cho SKS, et al. Redox ratio in the left ventricle of the growth restricted fetus is positively correlated with cardiac output. *J Biophotonics*. (2021) 14:e202100157. doi: 10.1002/jbio.202100157

41. Ren J, Darby JRT, Lock MC, Holman SL, Saini BS, Bradshaw EL, et al. Impact of maternal late gestation undernutrition on surfactant maturation, pulmonary blood flow and oxygen delivery measured by magnetic resonance imaging in the sheep fetus. *J Physiol*. (2021) 599:4705–24. doi: 10.1113/JP281292

42. Seed M. *In utero* brain development in fetuses with congenital heart disease: another piece of the jigsaw provided by blood oxygen level-dependent magnetic resonance imaging. *Circ Cardiovasc Imaging*. (2017) 10:e007181. doi: 10.1161/CIRCIMAGING.117.007181

43. Sun L, van Amerom JFP, Marini D, Portnoy S, Lee FT, Saini BS, et al. Characterization of hemodynamic patterns in human fetuses with cyanotic congenital heart disease using MRI. *Ultrasound Obstet Gynecol*. (2021) 58:824–36. doi: 10.1002/uog.23707

44. Sun L, Macgowan CK, Sled JG, Yoo SJ, Manlhiot C, Porayette P, et al. Reduced fetal cerebral oxygen consumption is associated with smaller brain size in fetuses with congenital heart disease. *Circulation*. (2015) 131:1313–23. doi: 10.1161/CIRCULATIONAHA.114.013051

45. Saini BS, Ducas R, Darby JRT, Marini D, Sun L, Macgowan CK, et al. Feasibility of MRI assessment of maternal-fetal oxygen transport and consumption relative to maternal position in healthy late gestational pregnancies. *J Physiol*. (2023) 601:5413–36. doi: 10.1113/JP285097

46. Grundy D. Principles and standards for reporting animal experiments in the journal of physiology and experimental physiology. *J Physiol*. (2015) 593:2547–9. doi: 10.1113/JP270818

47. Russell WMS, Burch RL. *The principles of humane experimental technique*. London: Methuen (1959). 238 p.

48. Varcoe TJ, Darby JRT, Gatford KL, Holman SL, Cheung P, Berry MJ, et al. Considerations in selecting postoperative analgesia for pregnant sheep following fetal instrumentation surgery. *Anim Front*. (2019) 9:60–7. doi: 10.1093/af/vfz019

49. Edwards LJ, Simonetta G, Owens JA, Robinson JS, McMillen IC. Restriction of placental and fetal growth in sheep alters fetal blood pressure responses to angiotensin II and captopril. *J Physiol*. (1999) 515:897–904. doi: 10.1111/j.1469-7793.1999.897ab.x

50. Morrison JL, Chien C, Gruber N, Rurak D, Riggs W. Fetal behavioural state changes following maternal fluoxetine infusion in sheep. *Brain Res Dev Brain Res*. (2001) 131:47–56. doi: 10.1016/S0165-3806(01)00255-3

51. Darby JRT, Saini BS, Soo JY, Lock MC, Holman SL, Bradshaw EL, et al. Subcutaneous maternal resveratrol treatment increases uterine artery blood flow in the pregnant ewe and increases fetal but not cardiac growth. *J Physiol*. (2019) 597:5063–77. doi: 10.1113/JP278110

52. Schrauben EM, Saini BS, Darby JRT, Soo JY, Lock MC, Stirrat E, et al. Fetal hemodynamics and cardiac streaming assessed by 4D flow cardiovascular magnetic resonance in fetal sheep. *J Cardiovasc Magn Reson*. (2019) 21:8. doi: 10.1186/s12968-018-0512-5

53. Duan AQ, Lock MC, Perumal SR, Darby JR, Soo JY, Selvanayagam JB, et al. Feasibility of detecting myocardial infarction in the sheep fetus using late gadolinium enhancement CMR imaging. *J Cardiovasc Magn Reson*. (2017) 19:69. doi: 10.1186/s12968-017-0383-1

54. Saini BS, Darby JRT, Portnoy S, Sun L, van Amerom J, Lock MC, et al. Normal human and sheep fetal vessel oxygen saturations by T_2 magnetic resonance imaging. *J Physiol*. (2020) 598:3259–81. doi: 10.1113/JP279725

55. Cho SKS, Darby JRT, Saini BS, Lock MC, Holman SL, Lim JM, et al. Feasibility of ventricular volumetry by cardiovascular MRI to assess cardiac function in the fetal sheep. *J Physiol*. (2020) 598:2557–73. doi: 10.1113/JP279054

56. Christen T, Bolar DS, Zaharchuk G. Imaging brain oxygenation with MRI using blood oxygenation approaches: methods, validation, and clinical applications. *AJNR Am J Neuroradiol*. (2013) 34:1113–23. doi: 10.3174/ajnr.A3070

57. Xu J, Duan AQ, Marini D, Lim JM, Keunen J, Portnoy S, et al. The utility of MRI for measuring hematocrit in fetal anemia. *Am J Obstet Gynecol*. (2020) 222:81.e1–81.e13. doi: 10.1016/j.ajog.2019.07.016

58. Giri S, Shah S, Xue H, Chung YC, Pennell ML, Guehring J, et al. Myocardial T_2 mapping with respiratory navigator and automatic nonrigid motion correction. *Magn Reson Med*. (2012) 68:1570–8. doi: 10.1002/mrm.24139

59. Stainsby JA, Wright GA. Partial volume effects on vascular T_2 measurements. *Magn Reson Med*. (1998) 40:494–9. doi: 10.1002/mrm.1910400322

60. Yushkevich PA, Piven J, Hazlett HC, Smith RG, Ho S, Gee JC, et al. User-guided 3D active contour segmentation of anatomical structures: significantly improved efficiency and reliability. *NeuroImage*. (2006) 31:1116–28. doi: 10.1016/j.neuroimage.2006.01.015

61. Baker PN, Johnson IR, Gowland PA, Hykin J, Harvey PR, Freeman A, et al. Fetal weight estimation by echo-planar magnetic resonance imaging. *Lancet*. (1994) 343:644–5. doi: 10.1016/S0140-6736(94)92638-7

62. Roelfsema NM, Hop WC, Boito SM, Wladimiroff JW. Three-dimensional sonographic measurement of normal fetal brain volume during the second half of pregnancy. *Am J Obstet Gynecol*. (2004) 190:275–80. doi: 10.1016/S0002-9378(03)00911-6

63. Robinson JS, Kingston EJ, Jones CT, Thorburn GD. Studies on experimental growth retardation in sheep. The effect of removal of a endometrial caruncles on fetal size and metabolism. *J Dev Physiol*. (1979) 1:379–98.

64. Morrison JL, Botting KJ, Dyer JL, Williams SJ, Thornburg KL, McMillen IC. Restriction of placental function alters heart development in the sheep fetus. *Am J Physiol Regul Integr Comp Physiol*. (2007) 293:R306–13. doi: 10.1152/ajpregu.00798.2006

65. Sun L, Macgowan CK, Portnoy S, Sled JG, Yoo SJ, Grosse-Wortmann L, et al. New advances in fetal cardiovascular magnetic resonance imaging for quantifying the distribution of blood flow and oxygen transport: potential applications in fetal cardiovascular disease diagnosis and therapy. *Echocardiography*. (2017) 34:1799–803. doi: 10.1111/echo.13760

66. Sun L, Marini D, Saini B, Schrauben E, Macgowan CK, Seed M. Understanding fetal hemodynamics using cardiovascular magnetic resonance imaging. *Fetal Diagn Ther*. (2020) 47:354–62. doi: 10.1159/000505091

67. McMillen IC, Adams MB, Ross JT, Coulter CL, Simonetta G, Owens JA, et al. Fetal growth restriction: adaptations and consequences. *Reproduction*. (2001) 122:195–204. doi: 10.1530/rep.0.1220195

68. Darby JRT, Varcoe TJ, Orgeig S, Morrison JL. Cardiorespiratory consequences of intrauterine growth restriction: influence of timing, severity and duration of hypoxaemia. *Theriogenology*. (2020) 150:84–95. doi: 10.1016/j.theriogenology.2020.01.080

69. Cetin I, Taricco E, Mando C, Radaelli T, Boito S, Nuzzo AM, et al. Fetal oxygen and glucose consumption in human pregnancy complicated by fetal growth restriction. *Hypertension*. (2020) 75:748–54. doi: 10.1161/HYPERTENSIONAHA.119.13727

70. Rudolph AM. Fetal and neonatal pulmonary circulation. *Annu Rev Physiol*. (1979) 41:383–95. doi: 10.1146/annurev.ph.41.030179.002123

71. Rudolph AM. Distribution and regulation of blood flow in the fetal and neonatal lamb. *Circ Res*. (1985) 57:811–21. doi: 10.1161/01.RES.57.6.811

72. Schrauben EM, Darby JRT, Saini BS, Holman SL, Lock MC, Perumal SR, et al. Technique for comprehensive fetal hepatic blood flow assessment in sheep using 4D flow MRI. *J Physiol*. (2020) 598:3555–67. doi: 10.1113/JP279631

73. Bellotti M, Pennati G, De Gasperi C, Bozzo M, Battaglia FC, Ferrazzi E. Simultaneous measurements of umbilical venous, fetal hepatic, and ductus venosus blood flow in growth-restricted human fetuses. *Am J Obstet Gynecol*. (2004) 190:1347–58. doi: 10.1016/j.ajog.2003.11.018

74. Kiserud T, Kessler J, Ebbing C, Rasmussen S. Ductus venosus shunting in growth-restricted fetuses and the effect of umbilical circulatory compromise. *Ultrasound Obstet Gynecol*. (2006) 28:143–9. doi: 10.1002/uog.2784

75. Tchirikov M, Rybakowski C, Huneke B, Schroder HJ. Blood flow through the ductus venosus in singleton and multifetal pregnancies and in fetuses with intrauterine growth retardation. *Am J Obstet Gynecol*. (1998) 178:943–9. doi: 10.1016/S0002-9378(98)70528-9

76. Gentili S, Morrison JL, McMillen IC. Intrauterine growth restriction and differential patterns of hepatic growth and expression of IGF1, PCK2, and HSDL1 mRNA in the sheep fetus in late gestation. *Biol Reprod*. (2009) 80:1121–7. doi: 10.1095/biolreprod.108.073569

77. Owens JA, Kind KL, Carbone F, Robinson JS, Owens PC. Circulating insulin-like growth factors-I and -II and substrates in fetal sheep following restriction of placental growth. *J Endocrinol*. (1994) 140:5–13. doi: 10.1677/joe.0.1400005

78. McMillen IC, Robinson JS. Developmental origins of the metabolic syndrome: prediction, plasticity, and programming. *Physiol Rev*. (2005) 85:571–633. doi: 10.1152/physrev.00053.2003

79. Soo JY, Wiese MD, Berry MJ, McMillen IC, Morrison JL. Intrauterine growth restriction may reduce hepatic drug metabolism in the early neonatal period. *Pharmacol Res*. (2018) 134:68–78. doi: 10.1016/j.phrs.2018.06.003

80. Soo JY, Wiese MD, Berry MJ, Morrison JL. Does poor fetal growth influence the extent of fetal exposure to maternal medications? *Pharmacol Res*. (2018) 130:74–84. doi: 10.1016/j.phrs.2018.02.001

81. McBride GM, Meakin AS, Soo JY, Darby JRT, Varcoe TJ, Bradshaw EL, et al. Intrauterine growth restriction alters the activity of drug metabolising enzymes in the maternal-placental-fetal unit. *Life Sci*. (2021) 285:120016. doi: 10.1016/j.lfs.2021.120016

82. McBride GM, Wiese MD, Soo JY, Darby JRT, Berry MJ, Varcoe TJ, et al. The impact of intrauterine growth restriction on cytochrome P450 enzyme expression and activity. *Placenta*. (2020) 99:50–62. doi: 10.1016/j.placenta.2020.07.012

83. McGillick EV, Orgeig S, Morrison JL. Regulation of lung maturation by prolyl hydroxylase domain inhibition in the lung of the normally grown and placentally restricted fetus in late gestation. *Am J Physiol Regul Integr Comp Physiol*. (2016) 310:R1226–43. doi: 10.1152/ajpregu.00469.2015

84. Orgeig S, Crittenden TA, Marchant C, McMillen IC, Morrison JL. Intrauterine growth restriction delays surfactant protein maturation in the sheep fetus. *Am J Physiol Lung Cell Mol Physiol*. (2010) 298:L575–83. doi: 10.1152/ajplung.00226.2009

85. Abbas G, Shah S, Hanif M, Shah A, Rehman AU, Tahir S, et al. The frequency of pulmonary hypertension in newborn with intrauterine growth restriction. *Sci Rep*. (2020) 10:8064. doi: 10.1038/s41598-020-65065-2

86. Giussani DA, Spencer JA, Moore PJ, Bennet L, Hanson MA. Afferent and efferent components of the cardiovascular reflex responses to acute hypoxia in term fetal sheep. *J Physiol*. (1993) 461:431–49. doi: 10.1113/jphysiol.1993.sp019521

87. Rudolph AM, Itskovitz J, Iwamoto H, Reuss ML, Heymann MA. Fetal cardiovascular responses to stress. *Semin Perinatol*. (1981) 5:109–21.

88. Gagnon R, Murotsuki J, Challis JR, Fraher L, Richardson BS. Fetal sheep endocrine responses to sustained hypoxemic stress after chronic fetal placental embolization. *Am J Phys*. (1997) 272:E817–23. doi: 10.1152/ajpendo.1997.272.5.E817

89. Kamitomo M, Alonso JG, Okai T, Longo LD, Gilbert RD. Effects of long-term, high-altitude hypoxemia on ovine fetal cardiac output and blood flow distribution. *Am J Obstet Gynecol*. (1993) 169:701–7. doi: 10.1016/0002-9378(93)90646-Z

90. Robinson JS, Jones CT, Kingston EJ. Studies on experimental growth retardation in sheep. The effects of maternal hypoxaemia. *J Dev Physiol*. (1983) 5:89–100.

91. Herrera EA, Rojas RT, Krause BJ, Ebensperger G, Reyes RV, Giussani DA, et al. Cardiovascular function in term fetal sheep conceived, gestated and studied in the hypobaric hypoxia of the Andean *altiplano*. *J Physiol*. (2016) 594:1231–45. doi: 10.1113/JP271110

92. Parer JT. The effect of acute maternal hypoxia on fetal oxygenation and the umbilical circulation in the sheep. *Eur J Obstet Gynecol Reprod Biol*. (1980) 10:125–36. doi: 10.1016/0028-2243(80)90090-8

93. Adams MB, Brown RE, Gibson C, Coulter CL, McMillen IC. Tyrosine hydroxylase protein content in the medulla oblongata of the foetal sheep brain increases in response to acute but not chronic hypoxia. *Neurosci Lett*. (2001) 316:63–6. doi: 10.1016/S0304-3940(01)02381-3

94. Danielson L, McMillen IC, Dyer JL, Morrison JL. Restriction of placental growth results in greater hypotensive response to alpha-adrenergic blockade in fetal sheep during late gestation. *J Physiol*. (2005) 563:611–20. doi: 10.1113/jphysiol.2004.080523

95. Darby JRT, Varcoe TJ, Holman SL, McMillen IC, Morrison JL. The reliance on alpha-adrenergic receptor stimuli for blood pressure regulation in the chronically hypoxaemic fetus is not dependent on post-ganglionic activation. *J Physiol*. (2021) 599:1307–18. doi: 10.1113/JP280693

96. Ruijtenbeek K, Le Noble FAC, Janssen GM, Kessels CG, Fazzi GE, Blanco CE, et al. Chronic hypoxia stimulates periarterial sympathetic nerve development in chicken embryo. *Circulation*. (2000) 102:2892–7. doi: 10.1161/01.CIR.102.23.2892

97. Rurak DW, Gruber NC. Increased oxygen consumption associated with breathing activity in fetal lambs. *J Appl Physiol Respir Environ Exerc Physiol*. (1983) 54:701–7. doi: 10.1152/jappl.1983.54.3.701

98. Boyle DW, Hirst K, Zerbe GO, Meschia G, Wilkening RB. Fetal hind limb oxygen consumption and blood flow during acute graded hypoxia. *Pediatr Res*. (1990) 28:94–100. doi: 10.1203/00006450-199008000-00004

99. Tchirikov M, Eisermann K, Rybakowski C, Schroder HJ. Doppler ultrasound evaluation of ductus venosus blood flow during acute hypoxemia in fetal lambs. *Ultrasound Obstet Gynecol*. (1998) 11:426–31. doi: 10.1046/j.1469-0705.1998.11060426.x

100. Tchirikov M, Schroder HJ, Hecher K. Ductus venosus shunting in the fetal venous circulation: regulatory mechanisms, diagnostic methods and medical importance. *Ultrasound Obstet Gynecol*. (2006) 27:452–61. doi: 10.1002/uog.2747

101. Paulick RP, Meyers RL, Rudolph CD, Rudolph AM. Venous responses to hypoxemia in the fetal lamb. *J Dev Physiol*. (1990) 14:81–8.

102. Paulick RP, Meyers RL, Rudolph CD, Rudolph AM. Hemodynamic responses to alpha-adrenergic blockade during hypoxemia in the fetal lamb. *J Dev Physiol*. (1991) 16:63–9.

103. Coceani F, Adeagbo AS, Cutz E, Olley PM. Autonomic mechanisms in the ductus venosus of the lamb. *Am J Phys*. (1984) 247:H17–24. doi: 10.1152/ajpheart.1984.247.1.H17

104. Lewis AB, Heymann MA, Rudolph AM. Gestational changes in pulmonary vascular responses in fetal lambs *in utero*. *Circ Res*. (1976) 39:536–41. doi: 10.1161/01.RES.39.4.536

105. Morrison JL, Berry MJ, Botting KJ, Darby JRT, Frasch MG, Gatford KL, et al. Improving pregnancy outcomes in humans through studies in sheep. *Am J Physiol Regul Integr Comp Physiol*. (2018) 315:R1123–53. doi: 10.1152/ajpregu.00391.2017

106. Zhang S, Barker P, Botting KJ, Roberts CT, McMillan CM, McMillen IC, et al. Early restriction of placental growth results in placental structural and gene expression changes in late gestation independent of fetal hypoxemia. *Physiol Rep*. (2016) 4:e13049. doi: 10.14814/phy2.13049

107. Varcoe TJ, Darby JRT, Holman SL, Bradshaw EL, Kuchel T, Vaughan L, et al. Fetal cardiovascular response to acute hypoxia during maternal anesthesia. *Physiol Rep*. (2020) 8:e14365. doi: 10.14814/phy2.14365

108. Sullender CT, Richards LM, He F, Luan L, Dunn AK. Dynamics of isoflurane-induced vasodilation and blood flow of cerebral vasculature revealed by multi-exposure speckle imaging. *J Neurosci Methods*. (2022) 366:109434. doi: 10.1016/j.jneumeth.2021.109434

109. McGillick EV, Orgeig S, Giussani DA, Morrison JL. Chronic hypoxaemia as a molecular regulator of fetal lung development: implications for risk of respiratory complications at birth. *Paediatr Respir Rev*. (2017) 21:3–10. doi: 10.1016/j.prrv.2016.08.011